

RESEARCH ARTICLE

Differential protein expression profile in the hypothalamic GT1-7 cell line after exposure to anabolic androgenic steroids

Freddyson J. Martínez-Rivera¹, Juliana Pérez-Laspiur², María E. Santiago-Gascot¹, Abner G. Alemán-Reyes³, Emanuel García-Santiago⁴, Yolanda Rodríguez-Pérez², Cristhian Calo-Guadalupe⁴, Inelia Otero-Pagán¹, Roxsana N. Ayala-Pagán³, Magdiel Martínez⁵, Yisel M. Cantres-Rosario⁶, Loyda M. Meléndez^{2,6}, Jennifer L. Barreto-Estrada^{1*}

1 Department of Anatomy and Neurobiology, Medical Sciences Campus, University of Puerto Rico, San Juan, Puerto Rico, United States of America, **2** Translational Proteomics Center-RCMI, Medical Sciences Campus, University of Puerto Rico, San Juan, Puerto Rico, United States of America, **3** Department of Biology, University of Puerto Rico, Río Piedras Campus, San Juan, Puerto Rico, United States of America, **4** Department of Biotechnology, Universidad del Este, Carolina, Puerto Rico, United States of America, **5** Department of Physiology and Biophysics, Medical Sciences Campus, University of Puerto Rico, San Juan, Puerto Rico, United States of America, **6** Department of Microbiology and Medical Zoology, Medical Sciences Campus, University of Puerto Rico, San Juan, Puerto Rico, United States of America

* jennifer.barreto1@upr.edu



OPEN ACCESS

Citation: Martínez-Rivera FJ, Pérez-Laspiur J, Santiago-Gascot ME, Alemán-Reyes AG, García-Santiago E, Rodríguez-Pérez Y, et al. (2017) Differential protein expression profile in the hypothalamic GT1-7 cell line after exposure to anabolic androgenic steroids. PLoS ONE 12(7): e0180409. <https://doi.org/10.1371/journal.pone.0180409>

Editor: Hubert Vaudry, Universite de Rouen, FRANCE

Received: July 2, 2016

Accepted: June 15, 2017

Published: July 18, 2017

Copyright: © 2017 Martínez-Rivera et al. This is an open access article distributed under the terms of the [Creative Commons Attribution License](https://creativecommons.org/licenses/by/4.0/), which permits unrestricted use, distribution, and reproduction in any medium, provided the original author and source are credited.

Data Availability Statement: All relevant data are within the paper and its Supporting Information files.

Funding: This work was funded by RTRN Small Grants Program (U54MD008149) <http://grants.rtrn.net/index.php/SMALLGRANTS20162017>, to JLBE; NIH –NCCR (2P20RR016470) <http://www.nems.nih.gov/teams/Pages/NCCR.aspx>, to JLBE; NIGMS (8P20GM103475)

Abstract

The abuse of anabolic androgenic steroids (AAS) has been considered a major public health problem during decades. Supraphysiological doses of AAS may lead to a variety of neuro-endocrine problems. Precisely, the hypothalamic-pituitary-gonadal (HPG) axis is one of the body systems that is mainly influenced by steroidal hormones. Fluctuations of the hormonal milieu result in alterations of reproductive function, which are made through changes in hypothalamic neurons expressing gonadotropin-releasing hormone (GnRH). In fact, previous studies have shown that AAS modulate the activity of these neurons through steroid-sensitive afferents. To increase knowledge about the cellular mechanisms induced by AAS in GnRH neurons, we performed proteomic analyses of the murine hypothalamic GT1-7 cell line after exposure to 17 α -methyltestosterone (17 α -meT; 1 μ M). These cells represent a good model for studying regulatory processes because they exhibit the typical characteristics of GnRH neurons, and respond to compounds that modulate GnRH *in vivo*. Two-dimensional difference in gel electrophoresis (2D-DIGE) and mass spectrometry analyses identified a total of 17 different proteins that were significantly affected by supraphysiological levels of AAS. Furthermore, pathway analyses showed that modulated proteins were mainly associated to glucose metabolism, drug detoxification, stress response and cell cycle. Validation of many of these proteins, such as GSTM1, ERH, GAPDH, PEBP1 and PDIA6, were confirmed by western blotting. We further demonstrated that AAS exposure decreased expression of estrogen receptors and GnRH, while two important signaling pathway proteins p-ERK, and p-p38, were modulated. Our results suggest that steroids have the capacity to directly affect the neuroendocrine system by modulating key cellular processes for the control of reproductive function.

<https://www.nigms.nih.gov/Pages/default.aspx> to JLBE; MBRS-RISE (R25GM061838) <http://mbrs-rise.rcm.upr.edu> to FJMR; MBRS-RISE (R25GM066250) http://www.suagm.edu/une/propuestas/riase/riase_index.html to EGS and CCG; RCMI Translational Proteomics Center NIMHD (8G12MD007600), http://rcmi.rcm.upr.edu/resreso/guidelines_rcmi. The funders had no role in study design, data collection and analysis, decision to publish, or preparation of the manuscript.

Competing interests: The authors have declared that no competing interests exist.

Introduction

The anabolic androgenic steroids (AAS) are synthetic derivatives of testosterone, created to provide anabolic potency and low androgenic effect [1]. While most users abuse AAS to improve physical performance, nearly all of them are unaware of the numerous side effects that can be associated with androgen misuse [2]. Cardiovascular diseases, cancer, liver dysfunction and psychiatric disorders are some of those well- documented problems [2,3]. Similarly, under the influence of AAS, the hypothalamic-pituitary-gonadal (HPG) axis is one of the most affected body systems [4,5]. The neural control of this axis resides within the hypothalamus, which is characterized by the expression of high levels of androgen and estrogen receptors (AR and ER) [6]. The medial preoptic area (mPOA) is a steroid-sensitive hypothalamic region, that is populated by neurons expressing gonadotropin-releasing hormone (GnRH) [7]. Indeed, GnRH neurons respond to fluctuations of gonadal steroids, which result in neuroplasticity changes leading to pulsatile secretion of this peptide. *In vivo* and *in vitro* studies have shown that exposure to steroids is associated with alterations on GnRH expression and secretion. For instance, studies in rodents [8], and cells [9,10] showed that exposure to either androgens or estrogens reduced GnRH transcripts.

To date, few studies have investigated the effect of AAS in GnRH neurons. In this regard, electrophysiological studies have shown that AAS modulate the activity of these cells [4,5]. For example, the AAS 17 α -methyltestosterone (17 α -meT; 7.5 mg/kg), increased presynaptic GABA_A receptor (GABA_AR) currents of mPOA steroid-sensitive neurons, resulting in inhibition of GnRH cells [4]. Similarly, female mice exposed to 17 α -meT (7.5 mg/kg), displayed a diestrus-like pattern activity in GnRH neurons through the suppression of presynaptic kisspeptin excitatory inputs from the anteroventral periventricular nucleus [5]. Although these studies demonstrated neuroendocrine modulation by AAS, there is still a lack of a complete protein profile on GnRH neurosecretory cells after AAS exposure, which has the potential to reveal specific alterations in regulatory processes of the reproductive axis. In this study, we characterized the proteomic profile of GnRH neurons after exposure to supraphysiological levels of 17 α -meT.

Given the scattered concentration of GnRH neurosecretory cells within the mPOA [11], and the difficulty to establish an *in vivo* approach to study these neurons [9], we used the murine immortalized cell line of GnRH-secreting hypothalamic neurons (GT1-7) [12]. Certainly, GT1-7 cells have been very useful in studying regulatory processes because they exhibit the typical characteristics of GnRH neurons, and respond to the same compounds that modulate GnRH secretion *in vivo* [13–15]. Moreover, evidence reveals that GT1-7 cells express AR [16,17], ER [18,19], and receptors for GABA (GABA_AR) [20], cellular properties that confer responsiveness to androgenic and estrogenic compounds.

The use of omics technologies has gained popularity to uncover the use of anabolic agents in human sports, animal husbandry [21], and aquaculture [22]. Indeed, proteomic analyses have been applied for the screening of steroid effects on body tissues such as prostate [23], gonads [22], breast [24], muscles [25] and blood components [26]. In this study, we used two-dimensional difference in gel electrophoresis (2D-DIGE) in combination with mass spectrometry and western blotting to profile the proteome of GnRH neurons. We hypothesized that 17 α -meT will modulate the expression of proteins associated with neuroendocrine regulation, synaptic plasticity, and cellular stress; key biological processes that might impact reproductive competence and integrity.

Materials and methods

Cell culture and reagents

GT1-7 cells were grown as previously described [12]. In brief, cells were maintained in DMEM (Mediatech, Manassas, VA) supplemented with 10% fetal bovine serum (FBS; Hyclone, Waltham, MA) and penicillin/streptomycin (Gibco, Grand Island, NY). Cells were grown in 25 cm culture flasks and maintained in a humidified incubator at 37°C and 5% CO₂. Each culture flask represents an independent biological replicate.

Drug

A 2D-DIGE experiment was performed using four independent biological replicates per treatment (Control: n = 4; AAS: n = 4). Before AAS exposure, cells were grown in steroid-free serum (Hyclone Waltham, MA) during the log-phase growth (70–80% confluency). Thereafter, four (4) samples were treated with a supraphysiological dose of the AAS, 17 α -methyltestosterone (17 α -meT: 1 μ M; Sigma, St. Louis, MO) for 48 h as previously described [27]. Control samples were treated with vehicle (30% cyclodextrin in 0.9% saline; Sigma, St. Louis, MO). 17 α -meT was chosen as the presence of the C17 methyl group reduces its aromatization to 17 β -estradiol [28], and inhibits aromatization [29,30]. As the normal level of testosterone in male serum is 1 X 10⁻⁸ M (0.01 μ M) [31,32], the regimen used in our experiment (1 μ M for 48 h) [27] reflects a chronic supraphysiological dose. Cell viability after AAS exposure was assessed by trypan blue exclusion assay as previously described with some modifications [33].

Caspase activity

Caspase 3 activity was measured using the Caspase-Glo[®] 3/7 (Promega Co., Madison, WI), in which 50,000 cells/well were initially seeded in a flat bottom 96-well plate. Cells were incubated with equal volumes of the reagent to the culture medium for 1 h, and a Varioskan Flash Reader (Thermo Fisher Scientific, Waltham, MA) was used to assess relative luminescence. Caspase 9 activity was measured using the Caspase-9 Fluorometric assay (R&D Systems, Inc. Minneapolis, MN). Each sample contained the cell lysate (100 μ g of protein in 50 μ L), 50 μ L of 2X reaction buffer, and 5 μ L of caspase 9 fluorometric substrate (LEHD-AFC). The reaction was incubated for 1 h at 37°C in a flat bottom 96-well microplate. Fluorescence signal was indicative of caspase activation, and it was measured on a fluorescent plate reader (Gemini Spectra-Max, Molecular Devices, CA, USA).

Proteomic analyses

Protein extraction and protein quantification. Cells were harvested after 48 h of AAS exposure. Lysis Buffer (7 M urea, 2 M thiourea, 4% CHAPS; GE Healthcare, Pittsburgh, PA) and a cocktail of protease inhibitors (BioVision, Inc., Milpitas, CA) were added to the cell pellets. Samples were centrifuged at 13,000 g for 15 min at 4°C. Supernatants containing the cellular protein fractions were recovered and protein extracts were purified by precipitation, using a 2-D Clean-Up Kit (GE Healthcare, Pittsburgh, PA). After precipitation, protein pellets were resuspended in cell lysis buffer (30 mM Tris-HCL pH = 8, 7 M urea, 2 M thiourea, 4% CHAPS). Protein concentration was measured using a 2-D Quant Kit (GE Healthcare, Pittsburgh, PA). Kits were used as suggested by manufacturer's instructions.

Sample labeling. Cy5 and Cy3 labeling for analytical gels: Five (5) μ g of total protein from GT1-7 cells samples (4 controls, 4 AAS) were speed-vacuum dried and resuspended in cell lysis buffer. Samples were reduced by incubation with 2 nM TCEP (tris-[2-carboxyethyl] phosphine hydrochloride; GE Healthcare, Pittsburgh, PA) at 37°C for 1 h and then labeled with 4

nM of Cy5 saturation dye (GE Healthcare, Pittsburgh, PA) for 30 min at 37°C. One volume sample buffer (7 M urea, 2 M thiourea, 4% CHAPS), pH3-10NL IPG buffer, and 130 mM DTT was added to the samples. An internal standard was prepared by pooling 5 µg total protein of each sample, mixed together, and then speed vacuum-dried. Protein pellet was resuspended with cell lysis buffer and reduced with 2nM TCEP per 5 µg protein for 1 h at 37°C. The proteins were labeled with 4 nM of Cy3 saturation dye per 5 µg protein for 30 min at 37°C. One volume sample buffer was added to the samples. Each 5 µg of sample labeled with Cy5 was mixed with 5 µg of internal standard labeled with Cy3. Rehydration buffer (7 M urea, 2 M thiourea, 2% CHAPS), and 60 mM DTT, pH 3-10NL IPG buffer was added to a final volume of 450 µl.

Cy3 labeling for preparative gels: A total of 250 µg of protein (31.25 µg/ sample) from samples represented in analytical gels were pooled, speed vacuum-dried, resuspended in 250 µl of cell lysis buffer and treated with TCEP for 1 h at 37°C. Protein (250 µg) was labeled with Cy3 saturation dye for 30 min at 37°C. To stop the reaction, sample buffer was added to a final volume of 450 µl.

2D-DIGE. First dimension was carried out with an Ettan IPGphor apparatus (GE Healthcare, Pittsburgh, PA). Samples were loaded on 24 cm long Immobiline DryStrips gels with non-linear immobilized pH gradient 3–10 by overnight rehydration. Each gel contained the internal standard and one of the samples (analytical gels, after saturation labeling) or pooled material in the case of the preparative gel strip. Isoelectric focusing was carried out at a constant temperature of 20°C with a total of 78.5 kVh. Before the second dimension, separation strips were incubated with an equilibration solution (50 mM Tris-HCL pH = 8.8, 6 M urea, 30% glycerol, 2% SDS, 0.01 bromophenol blue containing 100 mM DTT) for 15 min. Then, the strips were loaded on the top of pre-cast 12% polyacrylamide gels and fixed with 0.5% agarose. The second dimension was carried out with an Ettan DALTwelve Electrophoresis System (GE Healthcare, Pittsburgh, PA) at 20°C. Current was held constant to 12 mA per gel for an overnight period. On the next day, current was increased to 20 mA per gel until bromophenol blue mark the end of the gel. For visualization of protein spots, signals were collected at excitation wavelength for Cy3 and Cy5 labeled sample at 540 and 635 nm, respectively, using Ettan DIGE Imager (GE Healthcare, Pittsburgh, PA). Gels were scanned at 100 µm resolution and analyzed using DeCyder 2-D 6.5 software (GE Healthcare, Pittsburgh, PA). Using a 2 mm diameter tip, spots selected for protein identification after DeCyder statistical analysis ($P < 0.05$) were picked from the preparative gel by automatic Ettan Spot Picker (GE Healthcare, Pittsburgh, PA).

In-gel digestion. Spots picked from 2D-DIGE preparative gel were washed at RT with 200 µl of 50% acetonitrile and 50 mM ammonium bicarbonate solution for 1 h. Gel pieces were dried and then incubated with trypsin overnight digestion at 37°C. Resulting peptides were extracted using a mixture of 60% acetonitrile and 0.1% trifluoroacetic acid (TFA). Samples were dried and resuspended in 0.5% trifluoroacetic acid. All samples were desalted and purified using C18 ZipTips (EMD Millipore, Billerica, MA) according to manufacturer's recommendations and resuspended in 2% acetonitrile with 0.1% formic acid prior to liquid chromatography tandem mass spectrometry (LC-MS/MS) analysis.

Mass spectrometry and protein identification. Tryptic peptides were reconstituted in 40 µL of 0.1% TFA (v/v) in water: acetonitrile (95:5) and 4 µL was directly loaded at 4 µL/min for 7 min onto a custom-made trap column (100 µm I.D. fused silica with Kasil frit) containing 2 cm of 200Å, 5 µm Magic C18AQ particles (Bruker-Michrom, Auburn, CA). Peptides were eluted using a custom-made analytical column (75 µm I.D. fused silica) with gravity-pulled tip and packed with 25 cm 100Å, 5 µm Magic C18AQ particles (Bruker-Michrom, Auburn, CA). Peptides were eluted with a linear gradient from 100% solvent A (0.1% formic acid:acetonitrile

[95:05]) to 35% solvent B (acetonitrile containing 0.1% formic acid) in 30 min at 300 nL/min, using a Proxeon Easy nanoLC system directly coupled to a LTQ Orbitrap Velos mass spectrometer (Thermo Scientific, Waltham, MA). Data were acquired using a data-dependent acquisition routine of acquiring one mass spectrum from m/z 350–2000 in the Orbitrap (resolution 60,000) followed by tandem mass spectrometry scans in the LTQ linear ion trap of the 10 most abundant precursor ions found in the mass spectrum. Charge state rejection of singly charged ions and dynamic exclusion was utilized to minimize data redundancy and maximize peptide identification. The raw data files were processed into peak lists for database searching.

Database Searching of all MS/MS samples was performed using Mascot (Matrix Science, London, UK; version 2.3.02) and X! Tandem (The GPM, thegpm.org; version CYCLONE [2010.12.01.1]). Charge state deconvolution and deisotoping were not performed. X! Tandem was set up to search a subset of the SwissProt_012512 database and Mascot was set up to search the SwissProt_022212 database (selected for Mus., unknown version, 16531 entries) assuming the digestion enzyme trypsin. Mascot and X! Tandem were searched with a fragment ion mass tolerance of 0.50 Da and a parent ion tolerance of 15 PPM. Pyro-glu from E of the n-terminus, oxidation of methionine, acetylation of the n-terminus and iodoacetamide derivative of cysteine were specified in X! Tandem as variable modifications. Pyro-glu from E of the n terminus, oxidation of methionine, acetylation of the n-terminus, iodoacetamide derivative of cysteine and acrylamide adduct of cysteine were specified in Mascot as variable modifications.

Scaffold (version Scaffold_3.4.5, Proteome Software Inc., Portland, OR) was used to validate MS/MS based peptide and protein identifications. Peptide identifications were accepted if they could be established at greater than 80% probability, as specified by the Peptide Prophet algorithm [34]. Protein identifications were accepted if they could be established at greater than 90% probability and contained at least 2 identified peptides. Protein probabilities were assigned by the Protein Prophet algorithm [35]. Proteins that contained similar peptides and could not be differentiated based on MS/MS analysis alone were grouped to satisfy the principles of parsimony.

Networks and pathways analysis

Uniprot database (www.uniprot.org) was used to identify protein localization and function. Ingenuity pathways analysis (IPA) knowledge base (www.ingenuity.com) was used to identify predominant interaction networks and biological functions of differentially expressed proteins [36]. This software uses computational algorithms to identify networks consisting of proteins of interest and their interactions with other proteins in the knowledge base. The network scores (negative log of the P value) are calculated according to the fit of the network to the focus proteins. In addition, IPA knowledge base identifies global function and canonical pathways of the entire data set of proteins. The significance values for the canonical pathways are calculated by Fisher's exact test right-tailed. Specifically, this test compares the number of proteins that contribute in a given pathway or process, relative to the total number of occurrences of these proteins in all pathway annotations stored in the IPA knowledge base.

Validation of differential protein expression

Sample preparation. GT1-7 cells were grown as previously described in proteomic experiments. Cells were washed with ice-cold PBS, and lysed with CellLytic Mammalian Lysis/Extraction Reagent, supplemented with SIGMAFAST™ Protease Inhibitor Tablets (Sigma–Aldrich, MO). Extracts were maintained with constant agitation for 30 min at 4°C and then centrifuged for 20 min at 17,000 g. Supernatants were collected and used to determine total protein concentration using the Bradford Quick-Start Protein Assay (Bio-Rad Laboratories,

Hercules, CA). All procedures were performed at 4°C and samples were stored at -80°C for further protein extraction and western blotting.

Western blotting. Western blotting was performed as previously described [37], with some modifications. Equal amounts of whole protein extracts were suspended in 6x Laemmli Sample Buffer, heated, loaded, and then electrophoresed on Pre-Casted TGX-SDS gels (Bio-Rad, CA). Gels were transferred to nitrocellulose membranes using the Bio-Rad Turbo Trans-Blot apparatus. Membranes were blocked with 5% (w/v) non-fat milk in TBST [25 mM Tris-HCl, pH 7.4, 150 mM NaCl and 0.1% (v/v) Tween-20] overnight at 4°C and the appropriate primary antibodies were added overnight at 4°C. Membranes were then washed with TBST and probed with the corresponding horseradish peroxidase-conjugated (HRP) secondary antibodies at 22°C for 1 h. Blots were visualized using an enhanced chemiluminescence kit (Super-Signal Femto, Pierce, IL) and images were obtained using a VersaDoc 1000 system (Bio-Rad, CA). All Western blots were performed at least in triplicate from three independent experiments, and densitometry analyses were normalized to β -actin expression using NIH ImageJ (v1.47d). Data from Western blots is presented as mean \pm standard error of the mean (S.E.M.). Student's t-test analyses were employed and statistical significance was established as * $P \leq 0.05$; ** $P \leq 0.01$.

Antibodies. The following primary antibodies were used: mouse anti-ERH (1:1000), mouse anti-PDIA6/ERP (1:1000), rabbit anti-ER α (1:1500), goat anti-AR (1:1000) and rabbit anti-GnRH1 (1:1000) from Santa Cruz Biotechnology (SCBT), Dallas, TX; rabbit anti-GSTM1 (1:2000) from Thermo Scientific, Waltham, MA; rabbit anti-PEBP1/RKIP (1:1000), rabbit anti-GAPDH (G3P)-HRP conjugated (1:3000), rabbit anti-p-ERK (1:10000), rabbit anti-ERK (1:6000), rabbit anti-p-p38 MAPK (Thr180/Tyr182) (1:10000), rabbit anti-AKT (pan) (1:15000) and rabbit anti- β -actin HRP conjugated (1:3000) from Cell Signaling Technology (CST) Danvers, MA.

Results

Proteomic changes in GT1-7 cells after AAS treatment

To investigate the effect of a supraphysiological dose of AAS in the proteome of GT1-7 cells, we used 2D-DIGE analyses in extracts from vehicle and 17 α -meT treated cells. Before examining the proteome, we first demonstrated that 17 α -meT at 1 μ M did not affect cell viability at 48 h (Control: 92.07 ± 0.012 ; 17 α -meT: 92.82 ± 0.013 ; $p = 0.703$, unpaired t-test). Likewise, there were no AAS-induced apoptosis as indicated by caspase activity assays. Values of relative luminescence units for caspase 3 were: Control: $6.5 \times 10^6 \pm 2.99 \times 10^5$; 17 α -meT: $6.99 \times 10^6 \pm 1.29 \times 10^5$; $t_6 = 1.527$; $p = 0.177$; unpaired t-test. Values of relative fluorescence units for caspase 9 were: Control: 468.21 ± 31.54 ; 17 α -meT: 464.61 ± 22.02 ; $t_5 = 0.097$; $p = 0.926$, unpaired t-test.

A total of 6,045 protein spots were detected automatically in the master 2D gel image, of which 84 protein spots were differentially expressed at a p value < 0.05 . From those 84 spots, only 23 were distinguishable on the preparative gel and picked for protein identification by LC-MS/MS. For easy visualization, white arrows in Fig 1A show those 23 spots from a representative analytical gel. After DeCyder analysis, spot peaks were generated. Fig 1B and 1C show examples of overexpressed (spot 2674) and underexpressed (spot 5747) protein-containing spots, respectively, during vehicle or AAS treatment.

Tables 1 and 2 show overexpressed and underexpressed protein spots and their correspondent proteins that were differentially regulated after treatment with AAS. From those 23 recognized spots, 17 different proteins were identified. Two to four proteins were detected per protein spot collected. Top protein hits with the best Mascot scores were selected for validation as having major contribution to DIGE abundance data. UniProt database (www.uniprot.org)

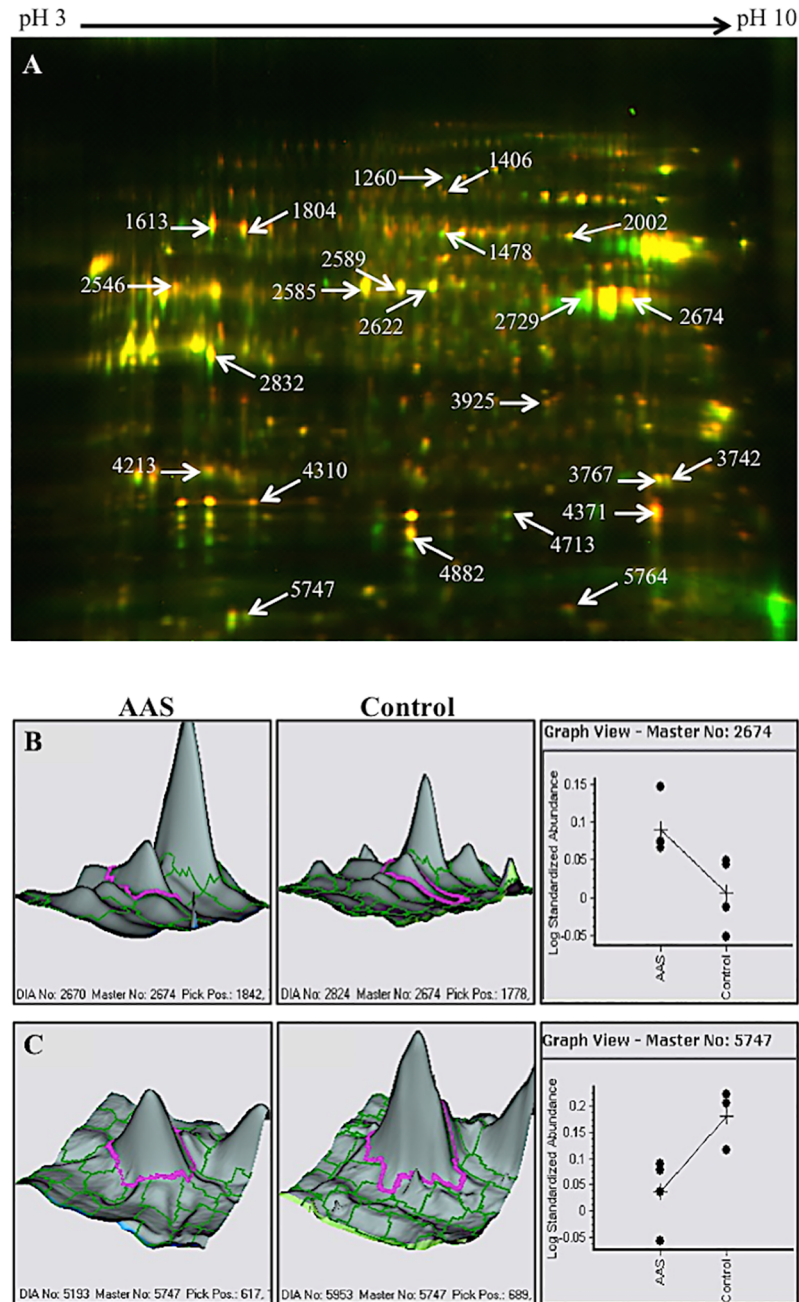


Fig 1. Representative images of 2D-DIGE analytical gel and 3D view of protein spots in vehicle and AAS-treated GT1-7 cells. (A) Twenty-three (23) protein spots were identified as differentially expressed in GT1-7 cells that were exposed to the AAS, 17 α -mE (1 μ M). Protein samples were labeled with Cy5 (red), whereas those from the internal standard were labeled with Cy3 (green). After merging, protein spots exhibiting no changes appear yellow in DIGE images, underexpressed proteins appear in green, and overexpressed proteins are in red. White numbers and arrows correspond to the identified proteins in Tables 1 and 2. (B-C) Panels depict the protein spots' abundance of (B) overexpressed and (C) underexpressed protein spots analyzed by DeCyder software. Purple lines encircle peaks representing protein spots from AAS-treated samples (left panels) or control vehicle (center panels). Protein abundance was calculated from normalized spot volume, standardized against the in-gel standard of each gel (right panels).

<https://doi.org/10.1371/journal.pone.0180409.g001>

Table 1. Overexpressed proteins in GT1-7 cells after AAS exposure.

Spot	^a Av. Ratio	P-Value	Gene	Description/Name	Accession no.	^b MW kDa	Peptides	Location	Function
4882	3.45	0.026	PPIA	Peptidyl-prolyl cis-trans isomerase A	P17742	18	9	Cytoplasm	Protein modification and binding
2832	1.88	0.02	SUCB2	Succinyl-CoA ligase [GDP-forming] subunit beta, mitochondrial	Q9Z2I8	47	4	Mitochondrion	Metabolism (Krebs cycle)
3742	1.51	0.043	GSTM1	Glutathione S-transferase Mu 1	P10649	26	3	Cytoplasm	Cellular detoxification
3742	1.51	0.043	GSTM2	Glutathione S-transferase Mu 2	P15626	26	7	Cytoplasm	Cellular detoxification
2729	1.45	0.045	G3P	Glyceraldehyde-3-phosphate dehydrogenase	P16858	36	10, 12	Cytoplasm	Metabolism (Glycolysis)
2674	1.21	0.035	(GAPDH)						
3925	1.42	0.047	PGAM1	Phosphoglycerate mutase 1	Q9DBJ1	29	8, 7	Cytoplasm	Metabolism (carbohydrate metabolism)
3767	1.26	0.015							
2002	1.42	0.045	STIP1	Stress-induced-phosphoprotein 1	Q60864	63	20	Cytoplasm/Nucleus	Stress response
2546	1.41	0.023	PDIA6 (ERP)	Protein disulfide-isomerase A6	Q922R8	48	11	Endoplasmic reticulum/cell membrane	Protein modification and binding
1613	1.37	0.014	HSP90B	Heat shock protein HSP 90-beta	P11499	83	26, 18	Cytoplasm	Stress response
1804	1.23	0.047							
1406	1.32	0.049	FLNA	Filamin-A	Q8BTM8	280	16	Cytoplasm	Cell motility
4371	1.32	0.031	COF1 (CFL)	Cofilin-1	P18760	18	5	Cytoplasm/cell membrane/nucleus	Cell cycle/cell motility
2585	1.27	0.013	ENOA (ENO1)	Alpha-enolase	P17182	47	14, 21, 23	Cytoplasm/cell membrane	Metabolism (carbohydrate metabolism)
2589	1.18	0.005							
2622	1.18	0.009							

^aAverage (Av) ratio represents the mean from four (4) different gels for both AAS-treated and control GT1-7 cells.

^bMolecular weight

<https://doi.org/10.1371/journal.pone.0180409.t001>

Table 2. Underexpressed proteins in GT1-7 cells after AAS exposure.

Spot	^a Av. Ratio	P-Value	Gene	Description/Name	Accession no.	^b MW kDa	Peptides	Location	Function
5747	-1.39	0.031	ERH	Enhancer of rudimentary homolog	P84089	12	5	Cell membrane	Cell cycle/RNA binding
1478	-1.50	0.0014	FLNA	Filamin-A	Q8BTM8	280	11	Cytoplasm	Cell motility
4713	-1.56	0.023	PPIA	Peptidyl-prolyl cis-trans isomerase A	P17742	18	4	Cytoplasm	Protein modification and binding
1260	-1.65	0.03	VINC (VCL)	Vinculin	Q64727	117	21	Cytoplasm/cell membrane	Cell motility
5764	-2.07	0.031	CX6A1	Cytochrome c oxidase subunit 6A1, mitochondrial	P43024	12	4	Mitochondrion	Metabolism/electron transport change
4213	-2.28	0.0021	VPS28	Vacuolar protein sorting-associated protein 28 homolog	Q9D1C8	25	3	Cell membrane/Cytoplasm	Protein transport
4310	-2.32	0.039	PEBP1	Phosphatidylethanolamine-binding protein 1	P70296	21	5	Cytoplasm	Nucleotide binding/Protease inhibitor

^aAverage (Av) ratio represents the mean from four (4) different gels for both AAS-treated and control GT1-7 cells.

^bMolecular weight

<https://doi.org/10.1371/journal.pone.0180409.t002>

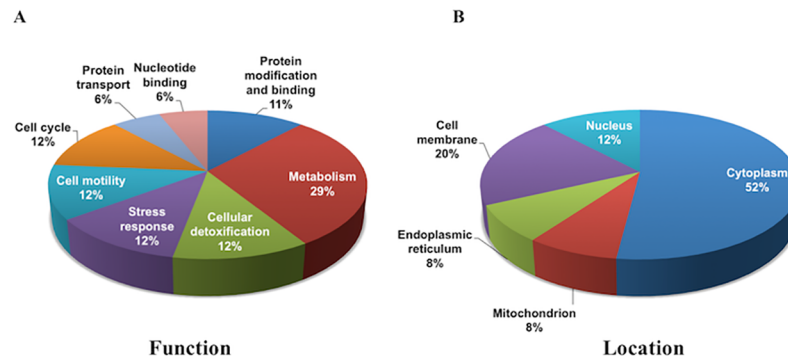


Fig 2. Cellular functions and locations of differentially expressed proteins in GT1-7 cells after AAS exposure. (A) A total of 8 biological processes with their respective cellular locations (B) were categorized from 17 different proteins identified by mass spectrometry. Data were obtained from Uniprot database (<http://www.uniprot.org>) and shown as percentages from the total number of proteins.

<https://doi.org/10.1371/journal.pone.0180409.g002>

revealed that differentially expressed proteins after AAS treatment are related to cellular metabolism, cell cycle, cell motility, stress response, drug detoxification, as well as protein and nucleotide processing or binding (Fig 2A). Subcellular location and biological function/process analysis revealed that the majority of the identified proteins were localized in the cytoplasm, cell membrane and nucleus (Fig 2B).

Overexpressed proteins in the category of glucose metabolism were: succinyl-CoA ligase [GDP-forming] subunit beta, mitochondrial (SUCB2), glyceraldehyde-3-phosphate dehydrogenase (GAPDH/G3P), phosphoglycerate mutase 1 (PGAM1), and alpha-enolase (ENOA). In this same category, cytochrome c oxidase subunit 6A1, mitochondrial (CX6A1) was underexpressed. In the category of cell motility, cofilin-1 (COF1) and vinculin (VCL) were found overexpressed and underexpressed, respectively. In proteins associated to cell cycle regulation, enhancer of rudimentary homolog (ERH) was underexpressed, while COF1 was also associated with this category. Other overexpressed proteins for the cellular stress response, were stress-induced-phosphoprotein 1 (STIP1) and heat shock protein HSP90-beta (HSP90B). Similar overexpression patterns were obtained for glutathione S-transferase Mu 1 & 2 (GSTM1 & 2), two key proteins associated with detoxification processes. On the other hand, overexpression of disulfide-isomerase A6 (PDIA6), a protein related to protein modification and binding, was also observed. In the category of transport-related proteins, vacuolar protein sorting-associated protein 28 homolog (VPS28) was found underexpressed. Finally, ERH, a protein linked to RNA binding and cell cycle, and phosphatidylethanolamine-binding protein 1 (PEBP1), a regulatory protein of nucleotide binding, were found underexpressed. Six proteins, FLNA, HSP90B, ENOA, G3P, PGAM and PPIA were represented in multiple spots and were also emphasized in Tables 1 and 2. From the 23 identified proteins, only two of them were found both overexpressed and underexpressed in different spots. These proteins were filamin (FLNA) and peptidyl-prolyl cis-trans isomerase A (PPIA), in the categories of cell motility and protein modification and binding, respectively.

Pathway analysis

Using the Ingenuity[®] Pathway Analysis software (IPA), we provided insights into AAS-induced protein expression changes in the GT1-7 cell line. These networks are ranked by scores, and are based on the number of focus proteins and the size of the network. Scores of 10 or higher (negative log of the P value) have high confidence, avoiding random effects [36]. The

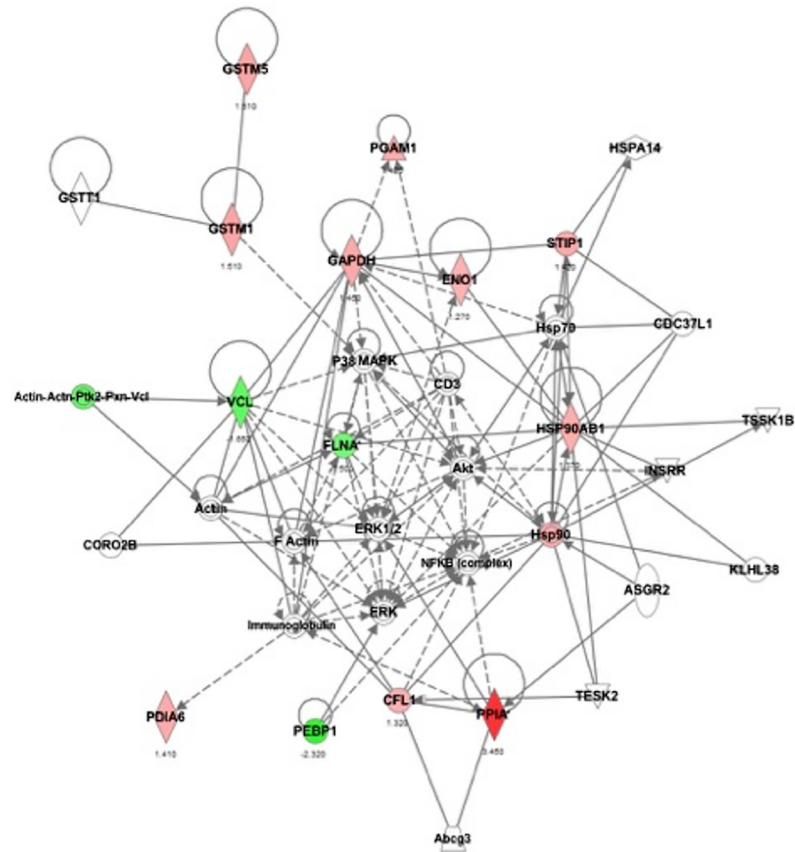


Fig 3. Network of proteins modulated by AAS in GT1-7 cells. Ingenuity Pathway Analysis (IPA) identified a major protein network associated with drug metabolism, glutathione depletion, protein synthesis, immunological disease and endocrine function. Red and green symbols indicate overexpressed and underexpressed proteins, respectively. GSTM2 is represented as GSTM5 in the IPA knowledge base. Direct interactions are represented as solid lines, whereas indirect interactions appear as dotted lines.

<https://doi.org/10.1371/journal.pone.0180409.g003>

pathway analysis identified only one network with a high score of 35, and it was associated to drug metabolism, glutathione depletion, protein synthesis, immunological disease, and endocrine system development and function. The network incorporated 13 focus proteins out of the 17 identified proteins modulated by 17 α -meT (Fig 3). The canonical signaling pathway showed the highest significance and number of focus proteins for glycolysis (3 proteins), gluconeogenesis (3 proteins), aryl hydrocarbon receptor (AHR signaling; 3 proteins), glutathione mediated detoxification (2 proteins) and NRF2-mediated oxidative stress response (3 proteins). Other signaling pathways associated with AAS-induced protein modulation are shown in Table 3.

Confirmation of proteomic changes by western blotting

In order to validate proteins that were differentially expressed in GT1-7 cells by AAS, we performed western blotting on cell lysates for several proteins in different categories. We found that all proteins tested by Western blots were expressed in GT1-7 cells. These were: GSTM1, GAPDH/G3P, ERH, PEBP1, and PDIA6. Thereafter, we performed Western blots to GT1-7 cell lysates in order to determine the expression of these proteins after steroid treatment. We confirmed that similar to the proteomic results, treatment with 17 α -meT increased the

Table 3. Canonical pathways modulated in GT1-7 cells after AAS exposure.

Pathway	-log (p-value)	Ratio	Molecules
Glycolysis	5.94E00	1.2E-01	ENO1, GAPDH, PGAM1
Gluconeogenesis	5.94E00	1.2E-01	ENO1, GAPDH, PGAM1
Aryl hydrocarbon receptor signaling	3.68E00	2.14E-02	GSTM1, GSTM2, HSP90B
Glutathione-mediated detoxification	3.54E00	6.67E-02	GSTM1, GSTM2
NRF2-mediated oxidative stress receptor	3.36E00	1.67E-02	GSTM1, GSTM2, STIP1
Actin cytoskeleton signaling	3.12E00	1.38E-02	CFL1, FLNA, VCL
Xenobiotic metabolism signaling	2.84E00	1.11E-02	GSTM1, GSTM2, HSP90B
NADH repair	2.6E00	3.33E-01	GAPDH
4-aminobutyrate degradation I	2.6E00	3.33E-01	SUCLG2 (SUCB2)
Rapoport-Luebering glycolytic shunt	2.47E00	2.5E-01	PGAM1
Glutamate degradation III (via 4-aminobutyrate)	2.37E00	2E-01	SUCLG2 (SUCB2)
ILK signaling	1.98E00	1.08E-02	CFL1, FLNA
LPS/IL-1 mediated inhibition of RXR function	1.84E00	9.13E-03	GSTM1, GSTM2
Maturity onset diabetes of young (MODY) signaling	1.73E00	4.55E-02	GAPDH
Mechanism of viral exit from host cells	1.47E00	2.44E-02	VPS28
Ephrin A signaling	1.4E00	2.08E-02	CFL1
Semaphorin signaling in neurons	1.36E00	1.89E-02	CFL1
Regulation of cellular mechanics by calpain protease	1.33E00	1.75E-02	VCL

Dataset generated by Ingenuity Pathway Analysis

<https://doi.org/10.1371/journal.pone.0180409.t003>

expression of GSTM1 and G3P (Fig 4A and 4B) and decreased expression of ERH and PEBP1 (Fig 4C and 4D). PDIA6 was observed to be underexpressed in Western blots, while 2D-DIGE revealed overexpression. Finally, in order to evaluate modulatory effects of AAS in classical endocrine substrates, we interrogated the expression of AR, ER and GnRH, as well as proteins associated to signaling pathway proteins (p-ERK, ERK, p-p38 and AKT). Densitometry analyses showed that 17 α -meT did not significantly change AR (Fig 5A), whereas ER (Fig 5B) and intracellular GnRH (Fig 5C) were decreased. Regarding the expression of signaling proteins, AAS exposure increased p-ERK expression (Fig 5D), while p-p38 (Fig 5E) was downregulated. On the other hand, expression of the non-phosphorylated forms, ERK and AKT did not change, as observed by the % of change over control (data not shown).

Discussion

The current study identified changes in the proteome of the hypothalamic GT1-7 cells in response to the synthetic androgen, 17 α -meT. Since physiological levels of androgens have been determined as 0.01 μ M [31,32], the dose regimen used in our study is considered a chronic supraphysiological (100-fold) exposure (1 μ M for 48 h) [27]. In fact, this steroid dosage reflects the regimen used by professional and amateur athletes who currently use 10 to 100-fold doses of AAS to improve their athletic performance [38–40]. In humans, although basal testosterone levels of cerebrospinal fluid (CSF) ranged between 0.0001–0.001 μ M [41,42], systemic exposure to high levels of methyltestosterone during 6 days (40–240 mg/day) led to concentrations in the CSF that ranged between 0.065–0.9 μ M [43]. This dose is similar to the dose tested in our *in vitro* study. These results suggest that cell populations in the brain of AAS abusers can be under the direct influence of supraphysiological concentrations of the drug, and that anabolic steroids have the potential to cause negative consequences at the molecular, physiological and/or behavioral levels.

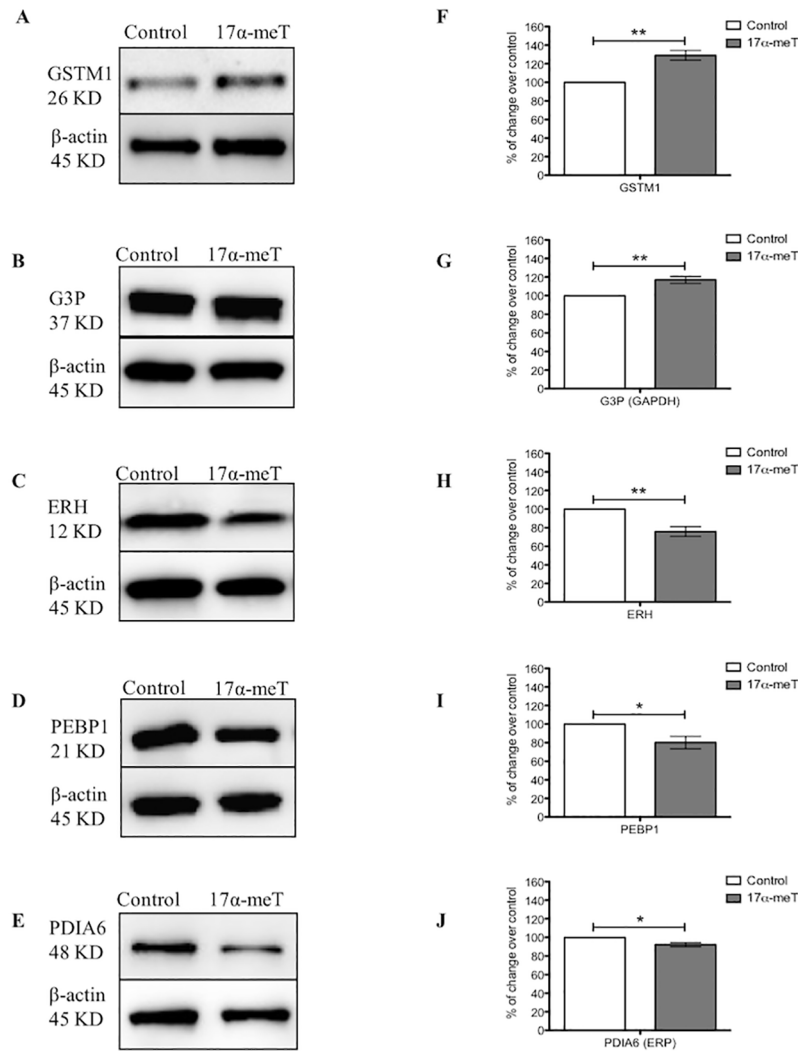


Fig 4. Validation of differentially expressed proteins in GT1-7 cells after AAS exposure. (A-E) Representative Western blots of identified proteins from protein extracts of AAS or vehicle-treated cells. **(F-J)** Densitometry analysis of each protein normalized to β -actin represents the relative protein expression values for **(A)** Glutathione S-transferase Mu 1 (GSTM1), **(B)** Glyceraldehyde 3-phosphate dehydrogenase (G3P/GAPDH), **(C)** Enhancer of rudimentary homolog (ERH), **(D)** Phosphatidylethanolamine-binding protein 1 (PEBP1), **(E)** Protein disulfide-isomerase A6/Endoplasmic Reticulum Protein (ERP/PDIA6). Error bars represent standard error of the mean. * $p \leq 0.05$, ** $p \leq 0.01$, unpaired t-test. $n =$ three replicates of three independent experiments for each group.

<https://doi.org/10.1371/journal.pone.0180409.g004>

Although androgen doses between 1 to 10 μ M initiated apoptosis in a neuroblastoma cell line [33], in our study, 1 μ M of AAS did not affect the viability of GT1-7 neurons, nor did they affect caspase activity. In this regard, two other cell lines have been differentially affected by androgens. Specifically, dopaminergic N27 neurons showed androgen-induced apoptosis, whereas GT1-7 cells were not affected [44]. Interestingly, others have shown that exposure to methandrostenolone (1 μ M), an AAS that belongs to the same category as 17 α -meT, reported cell viability that ranged between 80–95% [27]. To further argument against possible treatment-induced toxic effects, we showed that physiological levels of dihydrotestosterone (DHT, 0.1 μ M) overexpressed pERK (131.86% over control; $p = 0.026$, unpaired t-test), similar to what we observed by 17 α -meT (1 μ M). In accordance with our data, another study suggested

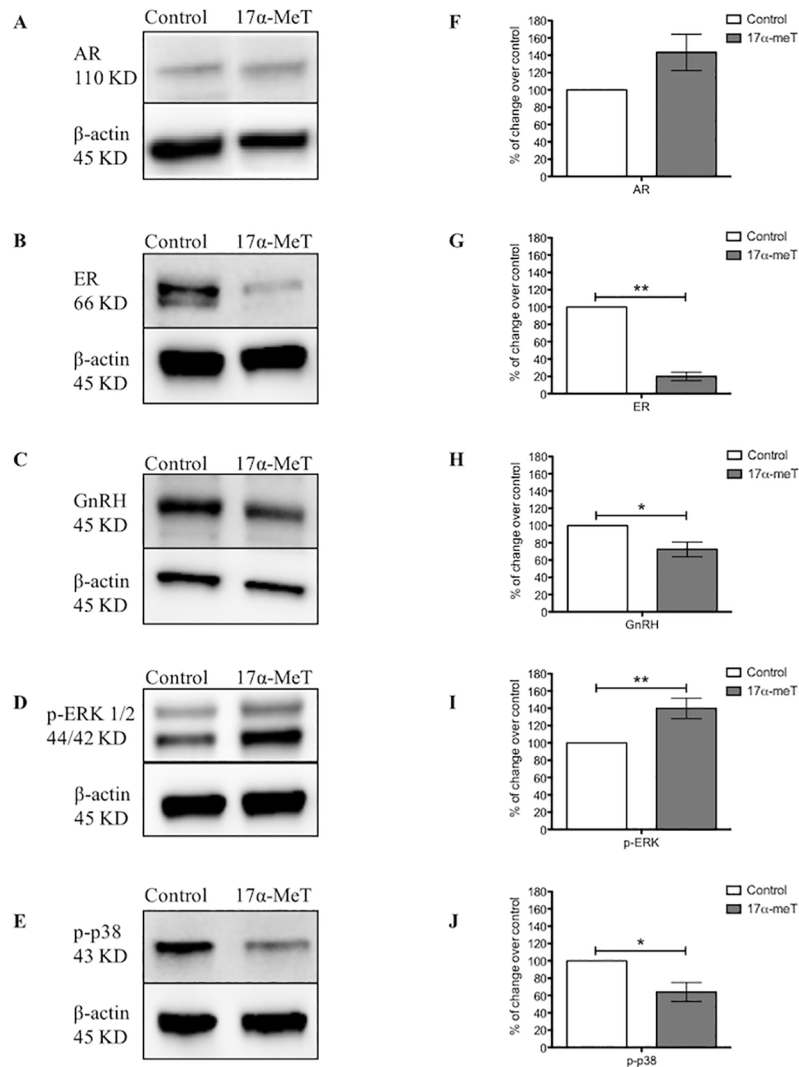


Fig 5. Protein expression of steroids receptors and signaling pathway proteins in GT1-7 cells after AAS exposure. (A-E) Representative Western blots of AR, ER, GnRH, p-ERK and p-p38 from protein extracts of AAS or vehicle-treated cells. (F-J) Densitometry analysis of each protein normalized to β -actin represents the relative protein expression values for (A) Androgen receptor (AR), (B) Estrogen receptor (ER), (C) GnRH, (D) Phospho-p44/42 MAPK (Erk1/2; Thr202/Tyr204), and (E) Phospho-p38 MAPK (p-p38), Error bars represent standard error of the mean. * $p < 0.05$, ** $p < 0.01$, unpaired t-test. $n =$ three replicates of three (AR and ER) or four (GnRH, p-ERK and p-p38) independent experiments for each group.

<https://doi.org/10.1371/journal.pone.0180409.g005>

that androgen-induced-neuroprotection might be achieved through overexpression/activation of ERK signaling [45]. Therefore, given that, in our study, the integrity of the cells was not compromised by a supraphysiological dose of androgens, we showed that, under these conditions, GT1-7 cells revealed protein changes in the categories of cellular metabolism, drug detoxification, stress response, cell cycle and motility, as well as in nucleotide binding and protein modification and transport.

Metabolism

In the metabolism category, the most significantly overexpressed proteins belong to the glycolysis and gluconeogenesis (5.94E00) pathways. In general, chronic exposure to androgens is

associated with insulin resistance, glucose intolerance, low glucose disposal rate and diabetes [46]. In neurons, increments in glycolytic enzymes are related to ion pumps recruitment, stimulation of glial glycolysis and glucose uptake [12,47]. In the rat epididymis, exposure to testosterone and DHT (1 mg/kg b.w.) increased the activity of GAPDH and PGAM [48]. Beside changes in metabolism, these proteins have been associated with other biological processes. For example, increased GAPDH expression has been linked to proliferation, apoptosis, cytoskeleton organization and synaptic remodeling [49]. Similarly, increments in ENOA and PGAM1 have been associated with tumor proliferation, cell migration, and apoptosis [50,51]. On the other hand, SUCB2, an enzyme of the tricarboxylic acid cycle (TCA) was found overexpressed, and associated by the canonical analysis with 4-aminobutyrate degradation I (2.6E00) and glutamate degradation III (via 4-aminobutyrate; 2.37E00). In this regard, others have shown that gene overexpression of TCA enzymes is related to high steroidogenic activity [52].

Drug detoxification and stress response

Regarding the possibility of 17α -meT inducing noxiousness and processes associating drug detoxification and stress response, we observed overexpression of two glutathione-mediated detoxification proteins (3.54E00), GSTM1 and GSTM2. GSTM proteins are steroid binding proteins characterized by their properties to bind testosterone and estradiol [53]. Upregulation of these antioxidant proteins has been related to drug insult, and detoxification of xenobiotics and oxidative products [54]. Interestingly, GSTM1 was upregulated by supraphysiological doses of DHT in peripheral human lymphocytes [26]. As well, corticosterone treatment in mice increased GSTM1 expression in steroid sensitive brain regions, such as the hypothalamus, hippocampus and cortex [36]. We also observed a modulation in the NRF2-mediated oxidative stress receptor pathway (3.36E00), associated with overexpression of the antioxidant and stress response proteins, GSTM and STIP1. This pathway has also been associated with a decreased expression of PEBP1, a Raf kinase inhibitory protein (RKIP). Therefore, it is not surprising that, in our study, PEBP1 was found to be decreased by 17α -meT.

The heat shock protein, HSP90B, was found overexpressed and associated with aryl hydrocarbon receptor (AHR; 3.68E00) and xenobiotic metabolism (2.84E00) pathways. HSP90B commonly acts as a chaperone molecule facilitating the proper folding of proteins in ATP-dependent reactions. This protein is also induced upon stress and xenobiotic exposure [55]. HSP90B also forms associations with AHR's and glucocorticoid receptors, which bind foreign compounds, including steroids [56]. Furthermore, AHR's may interact with a number of xenobiotic-binding proteins such as steroid receptors [56] and cytochrome P450, which also metabolize androgens [57], estrogens [58] and AAS [59].

Cell motility and cell cycle

Proteins related to cell motility and cytoskeleton dynamics were modulated after exposure to 17α -meT. This was represented by changes in VCL, FLNA, and CFL1 (3.12E00). VCL, a structural protein regulating cell-cell adhesion [60], showed decreased expression. Accordingly, the progesterone metabolite, 5 α -pregnane-3, 20-dione, decreases both VCL expression and cell adhesion, suggesting proliferative and metastatic inductions by an endogenous steroid [61]. Also, activation of androgen receptors correlates with VCL inhibition, restoring the migration potential of cancerous cells [62].

The scaffolding protein, FLNA, is linked to steroid-induced cell motility [63]. Although we observed this protein to be overexpressed and underexpressed in two different spots, which could suggest posttranslational modifications (PTM's) and isoform regulation, FLNA has been associated to the formation of complexes with androgen receptors in response to steroids. This

type of regulation has been documented in processes of neurogenesis, cell migration and invasiveness [64]. Additionally, FLNA facilitates nuclear translocation of the androgen receptor to modulate gene expression [65].

CFL1, a regulatory protein of mitosis and cell migration processes (www.uniprot.com), was found overexpressed after 17α -meT exposure. This protein acts through depolymerization of actin filaments by regulating the cytoskeleton dynamics and cell morphology [66]. Several reports indicate that steroids mediate the CFL1 phosphorylation pathway, inducing actin filament elongation [67]. Specifically, estrogen stimulates LIM kinase (LIMK)-dependent phosphorylation of CFL1, which promotes filopodial extensions and spine synapse growth. Increments in LIMK activity and CFL1 phosphorylation also correlate with cell proliferation [68] and migration [69].

ERH, another cell cycle protein, showed decreased expression in response to 17α -meT. Although the function of the protein is not well known, it has been associated to cell cycle, RNA binding/splicing and cancer processes [70]. ERH underexpression produces defects in chromosomal congression during mitosis [70,71]. Specifically, ERH depletion results in the loss of the mitotic motor protein, CENP-E, of the kinetochore, increasing mitosis duration. This depletion downregulates other genes involved in DNA replication and repair, suggesting that ERH is essential for chromosomal segregation and cell cycle progression [70,71]. Other experiments suggest that ERH underexpression may constrain tumor aggressiveness, given that ERH knockdown reduces tumor cell viability through KRAS oncogene-dependent pathways [70,72].

Protein modification and binding

PEBP1 (RKIP), a protease inhibitor, and also a protein related to nucleotide binding [73], was found underexpressed after exposure to 17α -meT. PEBP1 has been associated with suppression of metastasis [73]. Specifically, reduced expression of PEBP1 is highly associated to metastatic cancers, such as prostate metaplasia. Therefore, although a physiological dose of DHT (10 nM) increased PEBP1 expression in prostate epithelial cells [74], suggesting androgen anti-cancer properties, our results suggest that supraphysiological doses of steroids might induce detrimental tumorigenic and degenerative events.

PDIA6 and PPIA, two isomerases involved in protein modification and folding, were modulated in response to AAS treatment. Increased PDIA6 is associated to unfolded proteins response (UPR), a biological process that accumulates misfolded proteins in the endoplasmic reticulum, as a result of stress signals [75]. Although, 2D-DIGE analyses showed an overexpression of the spot containing PDIA6, a decreased was observed by western blotting. Discrepancies in both techniques have been previously reported [76,77], since 2D-DIGE detects PTM's and protein isoforms, whereas western blotting detects the overall protein signal [78]. Nonetheless, using 2D-DIGE, has been demonstrated that exposure to high testosterone doses overexpressed PDIA6 in rat meiotic spermatocytes [79]. Moreover, PPIA is associated with protein folding, lipid organization and stress response (www.uniprot.com). Although 17α -meT might be inducing PTMs on PPIA, as observed by over and underexpressed spots, increased expression of this protein has been related to dexamethasone [80] and estrogen [81] exposure.

Classical steroid receptors and GnRH signaling pathways

Previous studies demonstrated that exposure to androgens decreased GnRH in GT1-7 cells [9,12]. For instance, in these cells, several studies reported that DHT and testosterone (1–10 nM) [9,10,27], as well as DHEA (10^{-4} M), decreased GnRH transcript [28,82]. In the same line

of evidence, our data showed that 17α -meT decreased intracellular GnRH expression, suggesting repressive effects on FSH and LH, hormonal changes that might represent dysregulation of the endocrine system. However, we observed that 17α -meT caused a non-significant trend to increase AR expression. Similar to our results is the fact that DHT (2.4 μ M) did not modulate the expression of AR in lymphocytes [26]. While modulating proteins associated with cellular proliferation, cell death and drug metabolism. Interestingly, we found that AAS exposure decreased expression of ER, a result that is consistent with previous studies showing that, in the hypothalamus, its expression is inhibited by androgens [83].

Sex steroids have been found to modulate signal transduction pathways [84]. In this regard, p-ERK has been extensively related to cell proliferation, survival and plasticity [85,86]. While some studies suggest that androgens might reduce p-ERK expression and induce apoptosis [87], other studies demonstrate that testosterone activates p-ERK expression and proliferation [88,89]. The fact that we found proteins associated to cell proliferation, such as VCL, FLNA, GAPDH and STIP1, is in accordance with the proliferative effect of p-ERK. Therefore, it is suggested that these proteins might act as upstream regulators of ERK signaling pathways. Moreover, stimulation of cytoplasmic AR by anabolic steroids undergoes non-genomic signaling cascades leading to p-ERK activation and cell proliferation [90]. Interestingly, in our study, neither the non-phosphorylated forms of ERK nor AKT changed their expression after AAS exposure. On the other hand, the stress-activated kinase p-p38 [91] was downregulated, suggesting negative feedback for the restoration of cellular homeostasis after hormonal imbalance. This is in accordance with a previous study showing that acute stimulation of myotubes with supraphysiological doses of testosterone reduced phosphorylation of p38 MAPK [92].

Conclusion

By interrogating the proteome of the hypothalamic GT1-7 cell line as a model for studying AAS-induced regulatory processes of reproduction, we found that anabolic steroids modulate proteins associated to metabolism, cytoarchitecture, cellular homeostasis and hormonal regulation. Regarding possible direct androgen actions, it is worth mentioning that several of the identified proteins have androgen-response elements (ARE's). Specifically, the Androgen Responsive Gene Database (<http://argdb.fudan.edu.cn>) [93] revealed that proteins involved in metabolism (GAPDH, PGAM1, ENOA) stress response (STIP1, HSP90B) drug detoxification (GSTM1-2), protein modification (PEBP1, PPIA, PDIA6), and signaling pathway (ERK), contain ARE's. Although our findings provide a comprehensive molecular evaluation of how AAS might affect neurosecretory hypothalamic neurons, it is noteworthy to mention that *in vitro* studies using cell lines provide limitations when extrapolating results *in vivo*. Among the limitations in our study is the lack of complexity in the intact hypothalamic architecture, including afferent connections from distinct hypothalamic nuclei and neurons. In this scenario, it is still missing the neuronal interaction through neuropeptide/neurotransmitter signaling between GnRH neurons, feeding-related neurons and those from the suprachiasmatic nucleus. Despite these limitations, cell lines have proven themselves to be good models that are helpful in order to understand the *in vivo* complexity by providing a simpler system that is easy to maintain. This system has a homogeneous population of neurons, where controllable variables can be studied [94]. Therefore, differentially expressed proteins found in our study represent potential biomarkers of GnRH hypothalamic neurons for the detection of AAS-induced changes in reproductive function. It is then suggested that in steroid abusers, typical biological processes related to reproduction might be compromised through: i) activation of the biological machinery to reestablish cellular homeostasis after stressful and metabolic events, and/or ii) cellular

proliferation and migration that might induce tumorigenic activity. Future studies will be needed to test these modulated proteins against the physiology of reproduction.

Supporting information

S1 File. Western blot membranes and antibodies information for (A) GSTM1, (B) GP3/GAPDH, (C) ERH, (D) PEBP1, (E) PDIA6/ERP. Each antibody is normalized to β -actin (right panels).
(PDF)

S2 File. Western blot membranes and antibodies information for (A) AR, (B) ER, (C) GnRH, (D) p-ERK, (E) p-P38. Each antibody is normalized to β -actin (right panels).
(PDF)

Acknowledgments

This work was supported by grants, RCMC Translational Proteomics Center NIMHD (8G12MD007600), RTRN Small Grants Program (U54MD008149) to JLBE; NIH-NCRR (2P20RR016470) and NIGMS (8P20GM103475) to JLBE and MESG; MBRS-RISE (R25GM061838) to FJMR, and MBRS-RISE (R25GM066250) to EGS and CCG. Authors want to thank, Dr. Scott Shaffer, Director of Proteomics and Mass Spectrometry Facility at University of Massachusetts Medical School and Dr. Richard Noel, Director of Molecular and Genomics Core NIH-RCMI Program (NIMHD MD007579) at the Ponce Health Sciences University. We also thank Namyr Martínez for his technical assistance, and Angélica B. Rolón-Barreto for editorial revision.

Author Contributions

Conceptualization: JBE MSG FMR.

Formal analysis: JBE JPL FMR.

Funding acquisition: JBE LM.

Investigation: JBE FMR MSG JPL EG CCG AA IOP RAP YR.

Methodology: JBE JPL FMR MSG MM YCR.

Project administration: JBE.

Resources: JBE LM JPL YCR MM.

Supervision: JBE JPL.

Validation: FMR EG CCG AA IOP RAP.

Visualization: JBE.

Writing – original draft: FMR JBE JPL.

Writing – review & editing: FMR JBE.

References

1. Wood RI. Reinforcing aspects of androgens. *Physiol Behav.* 2004; 83: 279–289. <https://doi.org/10.1016/j.physbeh.2004.08.012> PMID: 15488545

2. Dodge T, Hoagland MF. The use of anabolic androgenic steroids and polypharmacy: A review of the literature. *Drug and alcohol dependence*. 2011. <https://doi.org/10.1016/j.drugalcdep.2010.11.011> PMID: [21232881](#)
3. van Amsterdam J, Opperhuizen A, Hartgens F. *Regulatory Toxicology and Pharmacology*. Regulatory Toxicology and Pharmacology. Elsevier Inc; 2010; 57: 117–123.
4. Penatti CAA, Davis MC, Porter DM, Henderson LP. Altered GABAA Receptor-Mediated Synaptic Transmission Disrupts the Firing of Gonadotropin-Releasing Hormone Neurons in Male Mice under Conditions That Mimic Steroid Abuse. *Journal of Neuroscience*. 2010; 30: 6497–6506. <https://doi.org/10.1523/JNEUROSCI.5383-09.2010> PMID: [20463213](#)
5. Penatti CAA, Oberlander JG, Davis MC, Porter DM, Henderson LP. Chronic exposure to anabolic androgenic steroids alters activity and synaptic function in neuroendocrine control regions of the female mouse. *Neuropharmacology*. 2011; 61: 653–664. <https://doi.org/10.1016/j.neuropharm.2011.05.008> PMID: [21645530](#)
6. Jin J-M, Yang W-X. Molecular regulation of hypothalamus–pituitary–gonads axis in males. *Gene*. 2014; 551: 15–25. <https://doi.org/10.1016/j.gene.2014.08.048> PMID: [25168889](#)
7. Moenter SM, DeFazio AnthonyR, Pitts GR, Nunemaker CS. Mechanisms underlying episodic gonadotropin-releasing hormone secretion. *Frontiers in Neuroendocrinology*. 2003; 24: 79–93. [https://doi.org/10.1016/S0091-3022\(03\)00013-X](https://doi.org/10.1016/S0091-3022(03)00013-X) PMID: [12762999](#)
8. Toranzo D, Dupont E, Simard J, Labrie C, Couet J, Labrie F, et al. Regulation of pro-gonadotropin-releasing hormone gene expression by sex steroids in the brain of male and female rats. *Mol Endocrinol*. 1989; 3: 1748–1756. <https://doi.org/10.1210/mend-3-11-1748> PMID: [2514347](#)
9. Belsham DD, Evangelou A, Roy D, Duc VL, Brown TJ. Regulation of gonadotropin-releasing hormone (GnRH) gene expression by 5alpha-dihydrotestosterone in GnRH-secreting GT1-7 hypothalamic neurons. *Endocrinology*. 1998; 139: 1108–1114. <https://doi.org/10.1210/endo.139.3.5846> PMID: [9492044](#)
10. Shakil T, Hoque ANE, Husain M, Belsham DD. Differential Regulation of Gonadotropin-Releasing Hormone Secretion and Gene Expression by Androgen: Membrane Versus Nuclear Receptor Activation. *Molecular Endocrinology*. 2002; 16: 2592–2602. <https://doi.org/10.1210/me.2002-0011> PMID: [12403848](#)
11. Schwanzel-Fukuda M, Jorgenson KL, Bergen HT, Weesner GD, Pfaff DW. Biology of Normal Luteinizing Hormone-Releasing Hormone Neurons During and After Their Migration from Olfactory Placode. *Endocrine Reviews*. 1992; 13: 623–634. <https://doi.org/10.1210/edrv-13-4-623> PMID: [1459046](#)
12. Mellon PL, Windle JJ, Goldsmith PC, Padula CA, Roberts JL, Weiner RI. Immortalization of hypothalamic GnRH neurons by genetically targeted tumorigenesis. *Neuron*. 1990; 5: 1–10. PMID: [2196069](#)
13. Gore AC, Roberts JL. Regulation of gonadotropin-releasing hormone gene expression in vivo and in vitro. *Frontiers in Neuroendocrinology*. 1997; 18: 209–245. <https://doi.org/10.1006/frne.1996.0149> PMID: [9101260](#)
14. Wetsel WC. Immortalized hypothalamic luteinizing hormone-releasing hormone (LHRH) neurons: a new tool for dissecting the molecular and cellular basis of LHRH physiology. *Cell Mol Neurobiol*. 1995; 15: 43–78. PMID: [7648609](#)
15. Wierman ME, Bruder JM, Kepa JK. Regulation of gonadotropin-releasing hormone (GnRH) gene expression in hypothalamic neuronal cells. *Cell Mol Neurobiol*. 1995; 15: 79–88. PMID: [7648611](#)
16. Brayman MJ, Pepa PA, Berdy SE, Mellon PL. Androgen Receptor Repression of GnRH Gene Transcription. *Molecular Endocrinology*. 2012; 26: 2–13. <https://doi.org/10.1210/me.2011-1015> PMID: [22074952](#)
17. Poletti A, Rampoldi A, Piccioni F, Volpi S, Simeoni S, Zanisi M, et al. 5Alpha-reductase type 2 and androgen receptor expression in gonadotropin releasing hormone GT1-1 cells. *J Neuroendocrinol*. 2001; 13: 353–357. PMID: [11264723](#)
18. Roy D, Angelini NL, Belsham DD. Estrogen directly respresses gonadotropin-releasing hormone (GnRH) gene expression in estrogen receptor-alpha (ERalpha)- and ERbeta-expressing GT1-7 GnRH neurons. *Endocrinology*. 1999; 140: 5045–5053. <https://doi.org/10.1210/endo.140.11.7117> PMID: [10537130](#)
19. Navarro CE, Saeed SA, Murdock C, Martinez-Fuentes AJ, Arora KK, Krsmanovic LZ, et al. Regulation of cyclic adenosine 3',5'-monophosphate signaling and pulsatile neurosecretion by Gi-coupled plasma membrane estrogen receptors in immortalized gonadotrophin-releasing hormone neurons. *Mol Endocrinol*. 2003; 17: 1792–1804.
20. Hales TG, Kim H, Longoni B, Olsen RW, Tobin AJ. Immortalized hypothalamic GT1-7 neurons express functional gamma-aminobutyric acid type A receptors. *Molecular Pharmacology*. 1992; 42: 197–202. PMID: [1325030](#)

21. Riedmaier I, Becker C, Pfaffl MW, Meyer HHD. The use of omic technologies for biomarker development to trace functions of anabolic agents. *Journal of Chromatography A*. 2009; 1216: 8192–8199. <https://doi.org/10.1016/j.chroma.2009.01.094> PMID: 19233374
22. Gao J, Liu S, Zhang Y, Yang Y, Yuan C, Chen S, et al. *Comparative Biochemistry and Physiology, Part D. Comparative Biochemistry and Physiology—Part D: Genomics and Proteomics*. Elsevier Inc; 2015; 15: 20–27.
23. Chen J, Huang P, Kaku H, Zhang K, Watanabe M, Saika T, et al. A comparison of proteomic profiles changes during 17beta-estradiol treatment in human prostate cancer PC-3 cell line. *Cancer Genomics Proteomics*. 2009; 6: 331–335. PMID: 20065320
24. Malorni L, Cacace G, Cuccurullo M, Pocsfalvi G, Chambery A, Farina A, et al. Proteomic analysis of MCF-7 breast cancer cell line exposed to mitogenic concentration of 17β-estradiol. *Proteomics*. 2006; 6: 5973–5982. <https://doi.org/10.1002/pmic.200600333> PMID: 17051647
25. Stella R, Biancotto G, Arrigoni G, Barrucci F, Angeletti R, James P. Proteomics for the detection of indirect markers of steroids treatment in bovine muscle. *Proteomics*. 2015; 15: 2332–2341. <https://doi.org/10.1002/pmic.201400468> PMID: 25757884
26. Imperlini E, Mancini A, Spaziani S, Martone D, Alfieri A, Gemei M, et al. Androgen receptor signaling induced by supraphysiological doses of dihydrotestosterone in human peripheral blood lymphocytes. *Proteomics*. 2010; 10: 3165–3175. <https://doi.org/10.1002/pmic.201000079> PMID: 20677326
27. Caraci F, Pistarà V, Corsaro A, Tomasello F, Giuffrida ML, Sortino MA, et al. Neurotoxic properties of the anabolic androgenic steroids nandrolone and methandrostenolone in primary neuronal cultures. *J Neurosci Res*. 2011; 89: 592–600. <https://doi.org/10.1002/jnr.22578> PMID: 21290409
28. Winters SJ. *Androgens: endocrine physiology and pharmacology*. NIDA Res Monogr. 1990; 102: 113–130. PMID: 2079969
29. de Gooyer ME, Oppers-Tiemissen HM, Leysen D, Verheul HAM, Kloosterboer HJ. Tibolone is not converted by human aromatase to 7α-methyl-17α-ethynylestradiol (7α-MEE). *Steroids*. 2003; 68: 235–243. [https://doi.org/10.1016/S0039-128X\(02\)00184-8](https://doi.org/10.1016/S0039-128X(02)00184-8) PMID: 12628686
30. Penatti CAA, Porter DM, Henderson LP. Chronic Exposure to Anabolic Androgenic Steroids Alters Neuronal Function in the Mammalian Forebrain via Androgen Receptor- and Estrogen Receptor-Mediated Mechanisms. *Journal of Neuroscience*. 2009; 29: 12484–12496. <https://doi.org/10.1523/JNEUROSCI.3108-09.2009> PMID: 19812324
31. Strauss RH, Lanese RR, Malarkey WB. Weight loss in amateur wrestlers and its effect on serum testosterone levels. *JAMA*. 1985; 254: 3337–3338. PMID: 4068168
32. Welder AA, Robertson JW, Melchert RB. Toxic effects of anabolic-androgenic steroids in primary rat hepatic cell cultures. *J Pharmacol Toxicol Methods*. 1995; 33: 187–195. PMID: 8527826
33. Estrada M, Varshney A, Ehrlich BE. Elevated Testosterone Induces Apoptosis in Neuronal Cells. *Journal of Biological Chemistry*. 2006; 281: 25492–25501. <https://doi.org/10.1074/jbc.M603193200> PMID: 16803879
34. Keller A, Nesvizhskii AI, Kolker E, Aebersold R. Empirical Statistical Model To Estimate the Accuracy of Peptide Identifications Made by MS/MS and Database Search. *Anal Chem*. 2002; 74: 5383–5392. <https://doi.org/10.1021/ac025747h> PMID: 12403597
35. Nesvizhskii AI, Keller A, Kolker E, Aebersold R. A Statistical Model for Identifying Proteins by Tandem Mass Spectrometry. *Anal Chem*. 2003; 75: 4646–4658. <https://doi.org/10.1021/ac0341261> PMID: 14632076
36. Skynner HA, Amos DP, Murray F, Salim K, Knowles MR, Munoz-Sanjuan I, et al. Proteomic analysis identifies alterations in cellular morphology and cell death pathways in mouse brain after chronic corticosterone treatment. *Brain Research*. 2006; 1102: 12–26. <https://doi.org/10.1016/j.brainres.2006.04.112> PMID: 16797492
37. Martínez-Rivera FJ, Natal-Albelo EJ, Martínez NA, Orozco-Vega RA, Muñoz-Seda OA, Barreto-Estrada JL. *Behavioural Processes*. Behavioural Processes. Elsevier B.V; 2015; 113: 81–85.
38. Yesalis CE, Bahrke MS. Anabolic-androgenic steroids. *Current issues*. *Sports Med*. 1995; 19: 326–340. PMID: 7618010
39. Payne JR. Cardiac effects of anabolic steroids. *Heart*. 2004; 90: 473–475. <https://doi.org/10.1136/hrt.2003.025783> PMID: 15084526
40. Frankenfeld SP, de Oliveira LP, Ignacio DL, Coelho RG, Mattos MN, Ferreira ACF, et al. Nandrolone decanoate inhibits gluconeogenesis and decreases fasting glucose in Wistar male rats. *Journal of Endocrinology*. 2014; 220: 143–153. <https://doi.org/10.1530/JOE-13-0259> PMID: 24403377
41. Mulchahey JJ, Ekhtor NN, Zhang H, Kasckow JW, Baker DG, Geraciotti TD. Cerebrospinal fluid and plasma testosterone levels in post-traumatic stress disorder and tobacco dependence. *Psychoneuroendocrinology*. 2001; 26: 273–285. PMID: 11166490

42. Stefansson J, Chatzittofis A, Nordström P, Arver S, Åsberg M, Jokinen J. CSF and plasma testosterone in attempted suicide. *Psychoneuroendocrinology*. 2016; 74: 1–6. <https://doi.org/10.1016/j.psyneuen.2016.08.009> PMID: 27567115
43. Daly RC, Su TP, Schmidt PJ, Pickar D, Murphy DL, Rubinow DR. Cerebrospinal fluid and behavioral changes after methyltestosterone administration: preliminary findings. *Arch Gen Psychiatry*. 2001; 58: 172–177. PMID: 11177119
44. Cunningham RL, Giuffrida A, Roberts JL. Androgens induce dopaminergic neurotoxicity via caspase-3-dependent activation of protein kinase Cdelta. *Endocrinology*. 2009; 150: 5539–5548. <https://doi.org/10.1210/en.2009-0640> PMID: 19837873
45. Nguyen T-VV, Yao M, Pike CJ. Androgens activate mitogen-activated protein kinase signaling: role in neuroprotection. *J Neurochem*. 2005; 94: 1639–1651. <https://doi.org/10.1111/j.1471-4159.2005.03318.x> PMID: 16011741
46. Cohen JC, Hickman R. Insulin resistance and diminished glucose tolerance in powerlifters ingesting anabolic steroids. *J Clin Endocrinol Metab*. 1987; 64: 960–963. <https://doi.org/10.1210/jcem-64-5-960> PMID: 3549761
47. Hall CN, Klein-Flugge MC, Howarth C, Attwell D. Oxidative Phosphorylation, Not Glycolysis, Powers Presynaptic and Postsynaptic Mechanisms Underlying Brain Information Processing. *Journal of Neuroscience*. 2012; 32: 8940–8951. <https://doi.org/10.1523/JNEUROSCI.0026-12.2012> PMID: 22745494
48. Brooks DE. Activity and androgenic control of glycolytic enzymes in the epididymis and epididymal spermatozoa of the rat. *Biochem J*. 1976; 156: 527–537. PMID: 182156
49. Colell A, Green DR, Ricci J-E. Novel roles for GAPDH in cell death and carcinogenesis. *Cell Death Differ*. Nature Publishing Group; 2009; 16: 1573–1581. <https://doi.org/10.1038/cdd.2009.137> PMID: 19779498
50. Fu Q-F, Liu Y, Fan Y, Hua S-N, Qu H-Y, Dong S-W, et al. Alpha-enolase promotes cell glycolysis, growth, migration, and invasion in non-small cell lung cancer through FAK-mediated PI3K/AKT pathway. 2015;: 1–13. <https://doi.org/10.1186/s13045-015-0117-5> PMID: 25887760
51. Hitosugi T, Zhou L, Elf S, Fan J, Kang H-B, Seo JH, et al. Phosphoglycerate Mutase 1 Coordinates Glycolysis and Biosynthesis to Promote Tumor Growth. *Cancer Cell*. 2012; 22: 585–600. <https://doi.org/10.1016/j.ccr.2012.09.020> PMID: 23153533
52. Hazard D, Liaubet L, SanCristobal M, Mormède P. Gene array and real time PCR analysis of the adrenal sensitivity to adrenocorticotrophic hormone in pig. *BMC Genomics*. 2008; 9: 101. <https://doi.org/10.1186/1471-2164-9-101> PMID: 18304307
53. Onaran I, Aydemir B, Kiziler AR, Demiryurek T, Alici B. Relationships between levels of estradiol and testosterone in seminal plasma and GSTM1 polymorphism in infertile men. *Arch Androl*. 2007; 53: 13–16. <https://doi.org/10.1080/01485010600889134> PMID: 17364458
54. Coles BF, Kadlubar FF. Detoxification of electrophilic compounds by glutathione S-transferase catalysis: determinants of individual response to chemical carcinogens and chemotherapeutic drugs? *Biofactors*. 2003; 17: 115–130. PMID: 12897434
55. Liu T, Pan L, Cai Y, Miao J. Molecular cloning and sequence analysis of heat shock proteins 70 (HSP70) and 90 (HSP90) and their expression analysis when exposed to benzo(a)pyrene in the clam *Ruditapes philippinarum*. *Gene*. Elsevier B.V.; 2015; 555: 108–118. <https://doi.org/10.1016/j.gene.2014.10.051> PMID: 25445266
56. Li H, Wang H. Activation of xenobiotic receptors: driving into the nucleus. *Expert Opin Drug Metab Toxicol*. 2010; 6: 409–426. <https://doi.org/10.1517/17425251003598886> PMID: 20113149
57. Zhang Y-Y, Yang L. Interactions between human cytochrome P450 enzymes and steroids: physiological and pharmacological implications. *Expert Opin Drug Metab Toxicol*. 2009; 5: 621–629. <https://doi.org/10.1517/17425250902967648> PMID: 19473111
58. Hwang K-A, Choi K-C. *Journal of Steroid Biochemistry & Molecular Biology*. Journal of Steroid Biochemistry and Molecular Biology. Elsevier Ltd; 2015; 147: 24–30.
59. Rendic S, Nolteernsting E, Schänzer W. Metabolism of anabolic steroids by recombinant human cytochrome P450 enzymes. Gas chromatographic-mass spectrometric determination of metabolites. *J Chromatogr B Biomed Sci Appl*. 1999; 735: 73–83. PMID: 10630892
60. Peng X, Nelson ES, Maiers JL, DeMali KA. New Insights into Vinculin Function and Regulation. *International Review of Cell and Molecular Biology*. Elsevier; 2011. pp. 191–231. <https://doi.org/10.1016/B978-0-12-386043-9.00005-0>
61. Wiebe JP, Muzia D. The endogenous progesterone metabolite, 5a-pregnane-3,20-dione, decreases cell-substrate attachment, adhesion plaques, vinculin expression, and polymerized F-actin in MCF-7 breast cancer cells. *Endocrine*. 2001; 16: 7–14. PMID: 11822829
62. Gu S, Papadopoulou N. *Mol Med*. 2011; 17: 1.

63. Castoria G, Giovannelli P, Di Donato M, Ciociola A, Hayashi R, Bernal F, et al. Role of non-genomic androgen signalling in suppressing proliferation of fibroblasts and fibrosarcoma cells. *Nature Publishing Group*; 2014; 5: e1548–12. <https://doi.org/10.1038/cddis.2014.497> PMID: 25476896
64. Castoria G, D'Amato L, Ciociola A, Giovannelli P, Giraldi T, Sepe L, et al. Androgen-Induced Cell Migration: Role of Androgen Receptor/Filamin A Association. AgoulNIK I, editor. *PLoS ONE*. 2011; 6: e17218. <https://doi.org/10.1371/journal.pone.0017218> PMID: 21359179
65. Ozanne DM, Brady ME, Cook S, Gaughan L, Neal DE, Robson CN. Androgen receptor nuclear translocation is facilitated by the f-actin cross-linking protein filamin. *Mol Endocrinol*. 2000; 14: 1618–1626. <https://doi.org/10.1210/mend.14.10.0541> PMID: 11043577
66. Bravo-Cordero JJ, Magalhaes MAO, Eddy RJ, Hodgson L, Condeelis J. Functions of cofilin in cell locomotion and invasion. *Nat Rev Mol Cell Biol*. 2013; 14: 405–417. <https://doi.org/10.1038/nrm3609> PMID: 23778968
67. Yuen GS, McEwen BS, Akama KT. LIM kinase mediates estrogen action on the actin depolymerization factor Cofilin. *Brain Research. Elsevier B.V.*; 2011; 1379: 44–52. <https://doi.org/10.1016/j.brainres.2010.07.067> PMID: 20696146
68. Zhang B, Yin C, Li H, Shi L, Liu N, Sun Y, et al. Nir1 promotes invasion of breast cancer cells by binding to chemokine (C–C motif) ligand 18 through the PI3K/Akt/GSK3b/Snail signalling pathway. *European Journal of Cancer. Elsevier Ltd*; 2013; 49: 3900–3913. <https://doi.org/10.1016/j.ejca.2013.07.146> PMID: 24001613
69. Wada-Kiyama Y, Suzuki C, Hamada T, Rai D, Kiyama R, Kaneda M, et al. Biochemical and Biophysical Research Communications. *Biochemical and Biophysical Research Communications. Elsevier Inc*; 2013; 434: 287–292.
70. Weng M-T, Luo J. The enigmatic ERH protein: its role in cell cycle, RNA splicing and cancer. *Protein Cell*. 2013; 4: 807–812. <https://doi.org/10.1007/s13238-013-3056-3> PMID: 24078386
71. Fujimura A, Kishimoto H, Yanagisawa J, Kimura K. Biochemical and Biophysical Research Communications. *Biochemical and Biophysical Research Communications. Elsevier Inc*; 2012; 423: 588–592.
72. Marcotte R, Brown KR, Suarez F, Sayad A, Karamboulas K, Krzyzanowski PM, et al. Essential Gene Profiles in Breast, Pancreatic, and Ovarian Cancer Cells. *Cancer Discovery*. 2012; 2: 172–189. <https://doi.org/10.1158/2159-8290.CD-11-0224> PMID: 22585861
73. Escara-Wilke J, Yeung K, Keller ET. Raf kinase inhibitor protein (RKIP) in cancer. *Cancer Metastasis Rev*. 2012; 31: 615–620. <https://doi.org/10.1007/s10555-012-9365-9> PMID: 22684368
74. Zhang H, Wu J, Keller JM, Yeung K, Keller ET, Fu Z. Transcriptional Regulation of RKIP Expression by Androgen in Prostate Cells. *Cell Physiol Biochem*. 2012; 30: 1340–1350. <https://doi.org/10.1159/000343323> PMID: 23095933
75. Tufo G, Jones AWE, Wang Z, Hamelin J, Tajeddine N, Esposti DD, et al. The protein disulfide isomerases PDIA4 and PDIA6 mediate resistance to cisplatin-induced cell death in lung adenocarcinoma. *Nature Publishing Group*; 2014; 21: 685–695. <https://doi.org/10.1038/cdd.2013.193> PMID: 24464223
76. Suehara Y, Kikuta K, Nakayama R, Fujii K, Ichikawa H, Shibata T, et al. Anatomic site-specific proteomic signatures of gastrointestinal stromal tumors. *Prot Clin Appl*. 2009; 3: 584–596. <https://doi.org/10.1002/prca.200800168>
77. Yamada M, Fujii K, Koyama K, Hirohashi S, Kondo T. The Proteomic Profile of Pancreatic Cancer Cell Lines Corresponding to Carcinogenesis and Metastasis. *J Proteomics Bioinform*. 2009; 02: 001–018. <https://doi.org/10.4172/jpb.1000057>
78. McNamara LE, Dalby MJ, Riehle MO, Burchmore R. Fluorescence two-dimensional difference gel electrophoresis for biomaterial applications. *Journal of The Royal Society Interface*. 2009; 7: S107–S118.
79. Stanton PG, Sluka P, Foo CFH, Stephens AN, Smith AI, McLachlan RI, et al. Proteomic Changes in Rat Spermatogenesis in Response to In Vivo Androgen Manipulation; Impact on Meiotic Cells. He B, editor. *PLoS ONE*. 2012; 7: e41718. <https://doi.org/10.1371/journal.pone.0041718> PMID: 22860010
80. Nishimura M, Koeda A, Suzuki E, Shimizu T, Kawano Y, Nakayama M, et al. Effects of prototypical drug-metabolizing enzyme inducers on mRNA expression of housekeeping genes in primary cultures of human and rat hepatocytes. *Biochemical and Biophysical Research Communications*. 2006; 346: 1033–1039. <https://doi.org/10.1016/j.bbrc.2006.06.012> PMID: 16777070
81. Schroder AL, Pelch KE, Nagel SC. Estrogen modulates expression of putative housekeeping genes in the mouse uterus. *Endocrine*. 2009; 35: 211–219. <https://doi.org/10.1007/s12020-009-9154-6> PMID: 19219570
82. Cui H, Lin S-YJ, Belsham DD. Evidence that dehydroepiandrosterone, DHEA, directly inhibits GnRH gene expression in GT1–7 hypothalamic neurons. *Molecular and Cellular Endocrinology*. 2003; 203: 13–23. [https://doi.org/10.1016/S0303-7207\(03\)00121-7](https://doi.org/10.1016/S0303-7207(03)00121-7) PMID: 12782399

83. Liu X, Shi H. Review Article Regulation of Estrogen Receptor. *International Journal of Endocrinology*. Hindawi Publishing Corporation; 2015;: 1–17.
84. Angele MK, Nitsch S, Knöferl MW, Ayala A, Angele P, Schildberg FW, et al. Sex-specific p38 MAP kinase activation following trauma-hemorrhage: involvement of testosterone and estradiol. *Am J Physiol Endocrinol Metab*. 2003; 285: E189–E196. <https://doi.org/10.1152/ajpendo.00035.2003> PMID: 12791604
85. Mebratu Y, Tesfaigzi Y. How ERK1/2 activation controls cell proliferation and cell death: Is subcellular localization the answer? *Cell Cycle*. 2009; 8: 1168–1175. <https://doi.org/10.4161/cc.8.8.8147> PMID: 19282669
86. Seger R, Krebs EG. The MAPK signaling cascade. *FASEB J*. 1995; 9: 726–735. PMID: 7601337
87. Zhao K-K, Cui Y-G, Jiang Y-Q, Wang J, Li M, Zhang Y, et al. European Journal of Obstetrics & Gynecology and Reproductive Biology. *European Journal of Obstetrics and Gynecology*. Elsevier Ireland Ltd; 2013; 171: 301–306.
88. Cheng J, Watkins SC, Walker WH. Testosterone Activates Mitogen-Activated Protein Kinase via Src Kinase and the Epidermal Growth Factor Receptor in Sertoli Cells. *Endocrinology*. 2007; 148: 2066–2074. <https://doi.org/10.1210/en.2006-1465> PMID: 17272394
89. Fix C, Jordan C, Cano P, Walker WH. Testosterone activates mitogen-activated protein kinase and the cAMP response element binding protein transcription factor in Sertoli cells. *Proc Natl Acad Sci USA*. 2004; 101: 10919–10924. <https://doi.org/10.1073/pnas.0404278101> PMID: 15263086
90. Liao RS, Ma S, Miao L, Li R, Yin Y, Raj GV. Androgen receptor-mediated non-genomic regulation of prostate cancer cell proliferation. *Translational Andrology and ...* 2013. <https://doi.org/10.3978/j.issn.2223-4683.2013.09.07> PMID: 26816736
91. Zarubin T, Jiahuai H. Activation and signaling of the p38 MAP kinase pathway. *Cell research*. 2005.
92. Garrido P, Salehzadeh F, Duque-Guimaraes DE, Al-Khalili L. Negative regulation of glucose metabolism in human myotubes by supraphysiological doses of 17 β -estradiol or testosterone. *Metab Clin Exp*. 2014; 63: 1178–1187. <https://doi.org/10.1016/j.metabol.2014.06.003> PMID: 25034385
93. Jiang M, Ma Y, Chen C, Fu X, Yang S, Li X, et al. Androgen-responsive gene database: integrated knowledge on androgen-responsive genes. *Molecular Endocrinology*. 2009; 23: 1927–1933. <https://doi.org/10.1210/me.2009-0103> PMID: 19762544
94. Mayer CM, Fick LJ, Gingerich S, Belsham DD. Hypothalamic cell lines to investigate neuroendocrine control mechanisms. *Frontiers in Neuroendocrinology*. 2009; 30: 405–423. <https://doi.org/10.1016/j.yfrne.2009.03.005> PMID: 19341762